

Cite this article as: Zhang Jianyu, Zhao Xiaojia, Wang Yanhui, et al. Interfacial Microstructure Evolution During Solid-Liquid Reaction in Cold-Rolled Ti/Al Laminated Composites[J]. Rare Metal Materials and Engineering, 2021, 50(07): 2375-2384.

ARTICLE

Interfacial Microstructure Evolution During Solid-Liquid Reaction in Cold-Rolled Ti/Al Laminated Composites

Zhang Jianyu¹, Zhao Xiaojia², Wang Yanhui¹, Chen Qing'an¹, Li Hezong¹, Chen Yayu¹

¹School of Mechanical and Equipment Engineering, Hebei University of Engineering, Handan 056038, China; ²Hebei Key Laboratory of Heterocyclic Compounds, Handan University, Handan 056005, China

Abstract: Cold-rolled Ti/Al laminated composites were annealed at 675~750 °C for different time with superfluous Ti and Al, and the interfacial microstructure evolution in Ti/Al laminated composites during annealing was investigated. The results indicate that the interfacial layer between Ti and Al consists of two sub-layers: a compact TiAl₃ sub-layer with the microstructure of many randomly oriented cracks filled with Al, and a granular TiAl₃ sub-layer with the microstructure of granular particles distributed in Al matrix. The thickness of the compact TiAl₃ sub-layer is stable at different annealing temperatures for different durations, but the thickness of the granular sub-layer increases with increasing the annealing temperature and duration. Furthermore, the average volume fraction of TiAl₃ phase in the interfacial layer at different temperatures decreases with increasing the duration. A reaction diffusion model, in which the TiAl₃ phase is regarded as the result of diffusion and chemical reaction, was established to evaluate the formation mechanism of the interfacial layer. Additionally, the dissolution of TiAl₃ phase into liquid Al was considered in the model. The calculated results indicate that the formation of TiAl₃ phase is governed by the chemical reaction, and the equivalent thickness of TiAl₃ phase in the interfacial layer obeys a linear relationship with annealing time, which is attributed to the rapid diffusion of Ti and Al atoms through the thin TiAl₃ compact sub-layer.

Key words: microstructure evolution; solid-liquid reaction; Ti/Al laminated composites; kinetics

Recently, Ti/TiAl₃ metal/intermetallic compound (IMC) laminated composites have attracted a substantial amount of interest owing to their excellent properties, such as relatively high yield strength at elevated temperatures, high oxidation-corrosion resistance, low density, and good dimensional stability^[1]. Various techniques have been used to obtain these types of materials, such as diffusion bonding^[2], rolling with annealing^[3], explosive welding with annealing^[4], and insert molding with annealing^[5]. In these methods, TiAl₃ IMC is synthesized by solid-solid reaction or solid-liquid reaction between Ti and Al. Owing to the low reaction temperature, the growth rate of TiAl₃ phase synthesized by Ti/Al solid-solid reaction is relatively slow, causing that the production efficiency of Ti/TiAl₃ laminated composites is relatively low when the required thickness of TiAl₃ phase is large. Compared with the Ti/Al solid-solid reaction, the Ti/Al solid-liquid

reaction has a greater potential for engineering applications due to its faster atomic diffusion speed and shorter IMC forming time.

To date, many studies focused on the formation mechanism and growth kinetics of the interfacial layer during Ti/Al solid-liquid reaction. The reports^[6-11] all showed that the interfacial layer is mainly composed of TiAl₃ and Al, but their interfacial layer formation mechanisms are inconsistent with each other. Furthermore, because the preparation methods of Ti/Al diffusion couple and the Ti/Al solid-liquid reaction conditions are quite different in previous studies, the kinetics parameters, such as the kinetics exponent, growth rate constant, and activation energy, vary widely. For instance, Sujata et al^[12] annealed the Ti/Al diffusion couples prepared by embedded technique at 700~900 °C for 0.25~4 h, and the results showed that both the mass per unit area of TiAl₃ phase and the

Received date: November 23, 2020

Foundation item: National Natural Science Foundation of China (51807047); Youth Top Talent Science and Technology Research Project of Hebei Province Universities (BJ2019003); S&T Program of Hebei (20373901D); Natural Science Foundation of Hebei Province of China (E2019402433); Research and Development Project of Science and Technology of Handan City of China (19422111008-19)

Corresponding author: Chen Yayu, Ph. D., Associate Professor, School of Mechanical and Equipment Engineering, Hebei University of Engineering, Handan 056038, P. R. China, Tel: 0086-310-3969382, E-mail: chenayayu@hebeu.edu.cn

Copyright © 2021, Northwest Institute for Nonferrous Metal Research. Published by Science Press. All rights reserved.

interfacial layer thickness obey a linear relationship with annealing time, and the activation energies for the growth of $TiAl_3$ phase and interfacial layer are 14.93 and 15.7 kJ/mol, respectively. Mackowiak et al.^[13] annealed the Ti/Al diffusion couples prepared by embedded technique at 700–920 °C for 1.5–9 h, and they found that the interfacial layer thickness and the dissolution thickness of Ti also obey a linear relationship with annealing time, and the activation energies for the growth of interfacial layer and the dissolution of Ti are 92.4 and 96.6 kJ/mol, respectively. Jiang et al.^[14] annealed the Ti/Al diffusion couples prepared by embedded technique at 800 °C, and the results showed that at the initial stage, the growth of interfacial layer is governed by chemical reaction and obeys the linear law; then the growth of interfacial layer is governed by diffusion and consistent with the parabolic law. Gurevich et al.^[15] studied the solid-liquid reaction behavior between Ti and Al in Ti/Al laminated composites prepared by explosive welding and annealing at 675–750 °C. The results show that at the initial stage, the growth of interfacial layer follows the linear law, and the growth rate of interfacial layer is very slow due to the oxide films as the diffusion barrier; then the growth rate of interfacial layer increases rapidly when the oxide films rupture, but the growth of the interfacial layer still obeys the linear law. Nie^[16] and Assari^[17] et al investigated the growth kinetics of the interfacial layer in Ti/Al laminated composites prepared by hot rolling and insert molding, respectively. But the growth of interfacial layer is not determined owing to the effect of oxide films. In summary, the formation mechanism and growth kinetics of interfacial layer need to be investigated further.

In the present work, the Ti/Al laminated composites were prepared by cold roll bonding to eliminate the effect of oxide films. The microstructure evolution during the solid-liquid reaction in cold-rolled Ti/Al laminated composites was investigated, and the formation mechanism and growth kinetics of Ti/Al interfacial layer were studied by quantitative methods.

1 Experiment

The raw materials used in this work were commercial Gr.1 Ti (purity of 99.6wt%, thickness of 1 mm) and pure Al 1050 (purity of 99.5wt%, thickness of 3 mm) sheets with dimensions of 200 mm×300 mm, and the chemical composition of Gr.1 Ti and Al 1050 sheets is shown in Table 1. The Ti sheet was annealed in vacuum heat treatment furnace at 650 °C for 40 min, then furnace-cooled to 200 °C, and subsequently air-cooled to room temperature. The Al sheet was annealed in common heat treatment furnace at 450 °C for 40 min, and then air-cooled to room temperature. The annealed Ti and Al sheets were etched with 10vol% HF and 10vol% NaOH, respectively, cleaned with acetone, and then roughened using steel brush to eliminate the surface contamination and prepare a work-hardened layer on the surface for good bonding. Then the treated Ti and Al sheets were stacked and then bonded by cold rolling with 4 rolling passes and total thickness reduction of 75%. The as-rolled Ti/Al laminated composites were cut into specimens of 10 mm×15 mm using the electro-discharge

Table 1 Chemical composition of Ti and Al sheets (wt%)

Gr.1 Ti	Fe	C	N	H	O	Ti	Others
Content	0.20	0.08	0.03	0.015	0.18	99.6	0.40
Al 1050	Si	Fe	Cu	Mn	Mg	Al	Others
Content	0.25	0.40	0.05	0.05	0.05	99.5	0.16

machining. The specimen was inserted into a stainless-steel mold, and then the mold with the specimen was suspended in the holder with Cu wire, as shown in Fig. 1a. The specimens were annealed in common heat treatment furnace at 675, 700, 725, and 750 °C and then air-cooled to room temperature. The annealing time was 2, 5, 10, 20, 30, 45, 60, and 90 min. To reach the holding temperature quickly for the specimen, the wall thickness of the mold was only 1 mm, and the size of the mold is shown in Fig. 1b.

The surfaces of all specimens for metallographic examination were obtained along the normal direction (ND)-rolling direction (RD) planes. The cross-sections of all specimens were mechanically ground using SiC abrasive papers (400#, 800#, and 2000#) and polished using diamond powder pastes (2.5 and 0.5 μm). To eliminate the influence of surface diffusion, the surface layer with a thickness of ~1 mm was removed by grinding and polishing. The microstructures of specimens were observed using scanning electron microscopy (SEM, Hitachi Su8220) equipped with energy dispersive spectroscopy (EDS) for identifying the chemical composition. The average thicknesses of interfacial layers were measured from the SEM images using image processing software. Three specimens were used under each annealing condition, and 50 individual values of the representative interfacial layer thickness were measured for each specimen to obtain the average thickness value. The phase structure was investigated using X-ray diffraction (XRD, Bruker D8 Advance), and Cu $K\alpha$ radiation of 40 kV was used with the scan range of 10°~120°, and scan rate of 4°/min.

2 Results and Discussion

2.1 Microstructure and phase composition of annealed Ti/Al laminated composites

Fig.2 shows SEM back-scattered electron image of the as-

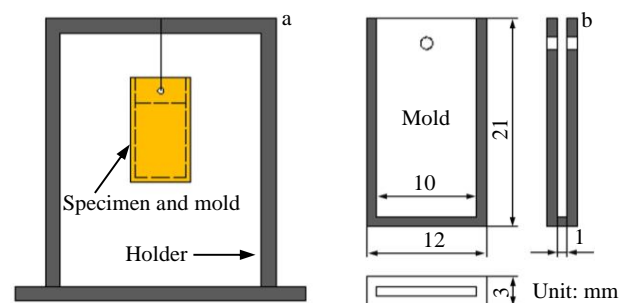


Fig.1 Schematic diagram of mold suspended on holder (a) and the dimensional size of mold (b)

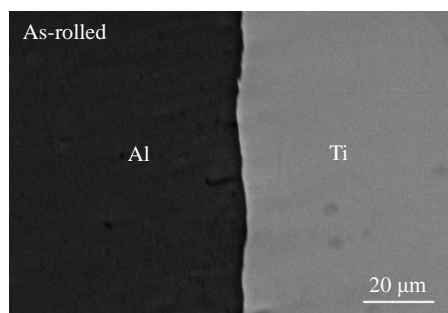


Fig.2 SEM back-scattered electron image of as-rolled Ti/Al laminated composite

rolled Ti/Al laminated composite. The dark region is identified as Al, the grey region is identified as Ti, and the thickness ratio of Al to Ti in the as-rolled Ti/Al laminated composite is approximately 3:1. The interface of the as-rolled Ti/Al laminated composite is well bonded with the fresh surface, and no IMCs form.

The microstructure evolutions in cold-rolled Ti/Al laminated composites annealed at 675~750 °C are similar, so only the SEM images of Ti/Al laminated composites annealed at 675 and 725 °C for different durations are shown in Fig.3. As shown in Fig.3a and 3b, after annealing for 2 min, the IMC layers of average thickness of 1.2 and 2.25 μm form at the interface of Ti/Al laminated composites, respectively. The interfacial layer forming at 725 °C is more uneven than that forming at 675 °C, and the granular particles are dispersed in Al matrix adjacent to the interfacial layer, indicating that the solid Al begins to melt. As shown in Fig.3c and 3d, after annealing for 5 min, the average thickness of interfacial layer in Ti/Al laminated composites annealed at 675 and 725 °C increases to 5.39 and 17.20 μm, respectively. Additionally, the granular particles are dispersed in Al matrix to form a granular

sub-layer, and randomly oriented cracks appear in the compact sub-layer adjacent to Ti, which are filled with Al. As shown in Fig.3e~3h, with increasing the annealing time, a small number of granular or irregular plate-like IMCs appear in Al matrix adjacent to the interfacial layer. The thickness of compact sub-layer in the interfacial layer is almost unchanged, but the thickness of granular sub-layer in the interfacial layer increases with increasing the annealing temperature or time. The size of most TiAl_3 particles in the granular sub-layer is 0~10 μm and increases slightly with increasing the annealing time.

The EDS results of different points in Fig.3 are shown in Table 2. It can be seen from the element content at point 1, 2, 4, and 6 that the IMCs in the granular and compact sub-layers are identified as TiAl_3 phase. The element content at point 3 and 7 shows that Ti hardly exists in Al solid solution due to the low solubility of Ti in Al solid solution^[18]. The element content at point 9 shows that Al hardly exists in Ti solid solution due to the low diffusion coefficient of Al in Ti solid solution^[19]. The higher Ti concentrations at point 5 and 8 are mainly caused by the TiAl_3 particles around Al solid solution. Therefore, the TiAl_3 particles beneath the metallographic surface of Al solid solution also play an important role. To further investigate the phase structure of Ti/Al laminated composites, XRD was performed using layer-by-layer method, i. e., the Al matrix and the granular sub-layer of the interfacial layer were removed layer-by-layer from the specimen using 10vol% NaOH solution. Fig.4 shows the XRD patterns from different surface layers of the specimens annealed at 725 °C for 60 min. As illustrated in Fig.4, only the diffraction peaks of Ti, Al, and TiAl_3 occur, indicating that IMC consists of only TiAl_3 phase.

2.2 Formation mechanism of interfacial layer in cold-rolled Ti/Al laminated composites

According to the Ti-Al binary alloy phase diagram^[18], IMCs, such as Ti_3Al , TiAl , TiAl_2 , and TiAl_3 , should form

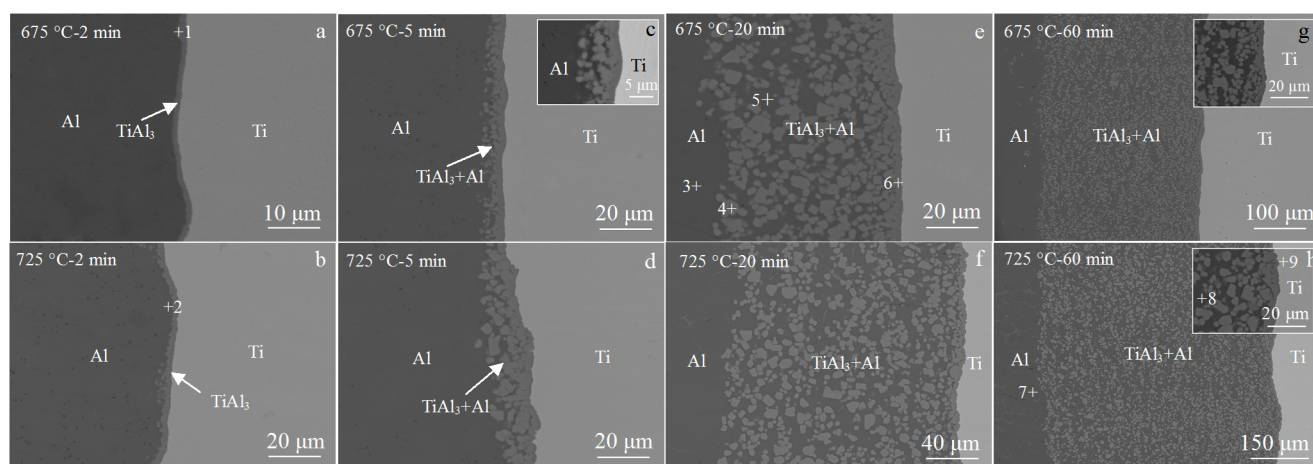


Fig.3 SEM images of cold-rolled Ti/Al laminated composites annealed at 675 °C (a, c, e, g) and 725 °C (b, d, f, h) for different time: (a, b) 2 min, (c, d) 5 min, (e, f) 20 min, and (g, h) 60 min (insets are detailed images of the corresponding compact sub-layers)

Table 2 EDS results of different points in Fig.3

Point	1	2	3	4	5	6	7	8	9
Al Content/at%	69.37	75.42	100	76.03	97.83	76.29	100	96.93	0
Ti Content/at%	30.63	24.58	0	23.97	2.17	23.71	0	3.07	100
Predicted phase	TiAl ₃	TiAl ₃	Al	TiAl ₃	Al	TiAl ₃	Al	Al	Ti

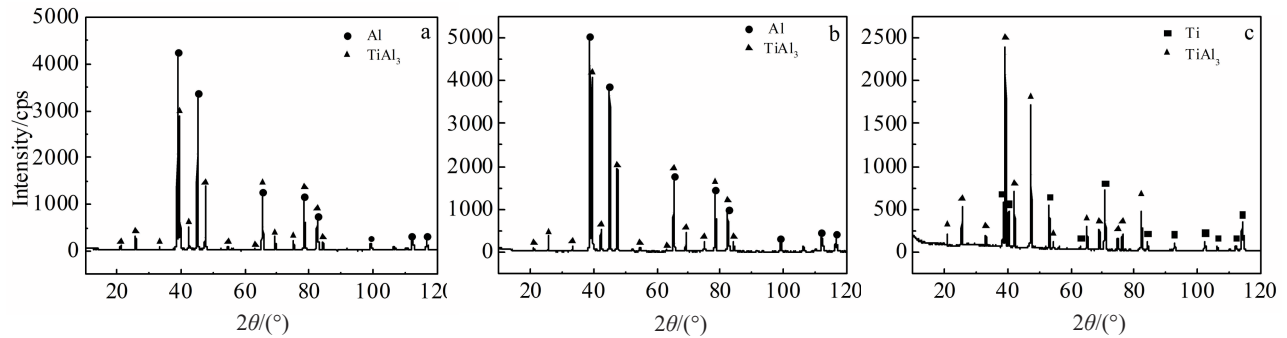


Fig.4 XRD patterns of different surface layers in Ti/Al laminated composites annealed at 725 °C for 60 min: (a) Al matrix surface, (b) granular sub-layer surface, and (c) compact sub-layer surface

between Ti and Al. However, it can be seen from the experiment results that only TiAl₃ phase forms in the Al-rich environment regardless of Ti/Al solid-solid reaction or Ti/Al solid-liquid reaction, which is attributed to the lower effective heat of formation and faster growth rate, compared with those of other Ti-Al IMCs^[17,20]. The formation mechanism of the interfacial layer in cold-rolled Ti/Al laminated composites during annealing and cooling is discussed as follows.

2.2.1 Solid-solid reaction between Ti and Al

After the specimen is put into the electric resistance furnace, the temperature of the specimen increases from room temperature to the holding temperature quickly within a few minutes owing to the thin mold wall, and the Ti/Al solid-solid reaction occurs before solid Al melts. Therefore, the Ti/Al solid-solid reaction mechanism is that the interdiffusion of Ti and Al atoms at interface generates the Al-rich and Ti-rich solid solution near interface. When the penetration depth of Ti in Al solid solution or that of Al in Ti solid solution achieves a certain value, the nucleation and lateral growth of TiAl₃ phase occur^[21]. Due to the thin oxide films of Ti and Al fully dispersed at the interface of cold-rolled Ti/Al laminated composites^[22] and the large diffusion coefficient of Ti in the Al solid solution (1.23×10^{-15} m²/s at 650 °C)^[23], TiAl₃ phase nucleates in a very short time. With increasing the annealing temperature or duration, the TiAl₃ phase gradually thickens along the direction perpendicular to the interface, as shown in Fig.5a.

2.2.2 Solid-liquid reaction between Ti and unsaturated Al

With increasing the annealing time, Al changes from solid into liquid. As shown in Fig. 5b, Ti and Al atoms diffuse through the thin TiAl₃ compact sub-layer along the opposite directions, and then TiAl₃ phase forms according to the chemical reaction in Eq. (1) between Ti and Al at the Ti/TiAl₃ (I) and TiAl₃/Al (II) interfaces:



Because liquid Al is unsaturated, TiAl₃ phase dissolves into liquid Al at TiAl₃/Al interface simultaneously. Therefore, the actual growth rate of TiAl₃ phase is the difference between the formation rate and the dissolution rate, which can be expressed by Eq.(2) as follows^[24]:

$$\frac{dx}{dt} = \left(\frac{dx}{dt}\right)_{\text{formation}} - \left(\frac{dx}{dt}\right)_{\text{dissolution}} \quad (2)$$

The formation rate of TiAl₃ phase can be expressed by Eq.(3) as follows:

$$\left(\frac{dx}{dt}\right)_{\text{formation}} = \frac{k_c^I}{1 + \frac{k_c^I x}{k_d^I}} + \frac{k_c^{II}}{1 + \frac{k_c^{II} x}{k_d^{II}}} \quad (3)$$

where k_c^I and k_c^{II} are the chemical reaction constants for the growth of TiAl₃ layer at interfaces I and II, respectively; k_d^I and k_d^{II} are the diffusion constants for the growth of TiAl₃ layer at interfaces I and II, respectively; x is the thickness of TiAl₃ compact sub-layer; t is the annealing duration. When $k_c^I \ll k_d^I/x$ and $k_c^{II} \ll k_d^{II}/x$, the growth of TiAl₃ phase is governed by chemical reaction; when $k_c^I \gg k_d^I/x$ and $k_c^{II} \gg k_d^{II}/x$, the growth of TiAl₃ phase is governed by diffusion. The dissolution rate of TiAl₃ phase can be expressed by the Nernst equation^[24], i.e., Eq. (4). According to the integration result of Eq. (4) with the initial condition of $x=0$ at $t=0$, the dissolved thickness of TiAl₃ phase x_d can be expressed by Eq.(5) as follows:

$$\left(\frac{dx}{dt}\right)_{\text{dissolution}} = \frac{c_s k}{\rho_{\text{TiAl}_3} \phi} \exp\left(-\frac{kSt}{V}\right) \quad (4)$$

$$x_d = \frac{c_s V}{\rho_{\text{TiAl}_3} \phi S} \left[1 - \exp\left(-\frac{kSt}{V}\right)\right] \quad (5)$$

where c_s is the solubility of Ti in liquid Al at a given temperature (c_s of 0.17wt%, 0.22wt%, 0.27wt%, and 0.33wt% Ti in liquid Al is 4.59, 5.94, 7.29, and 8.91 kg/m³ at 675, 700,

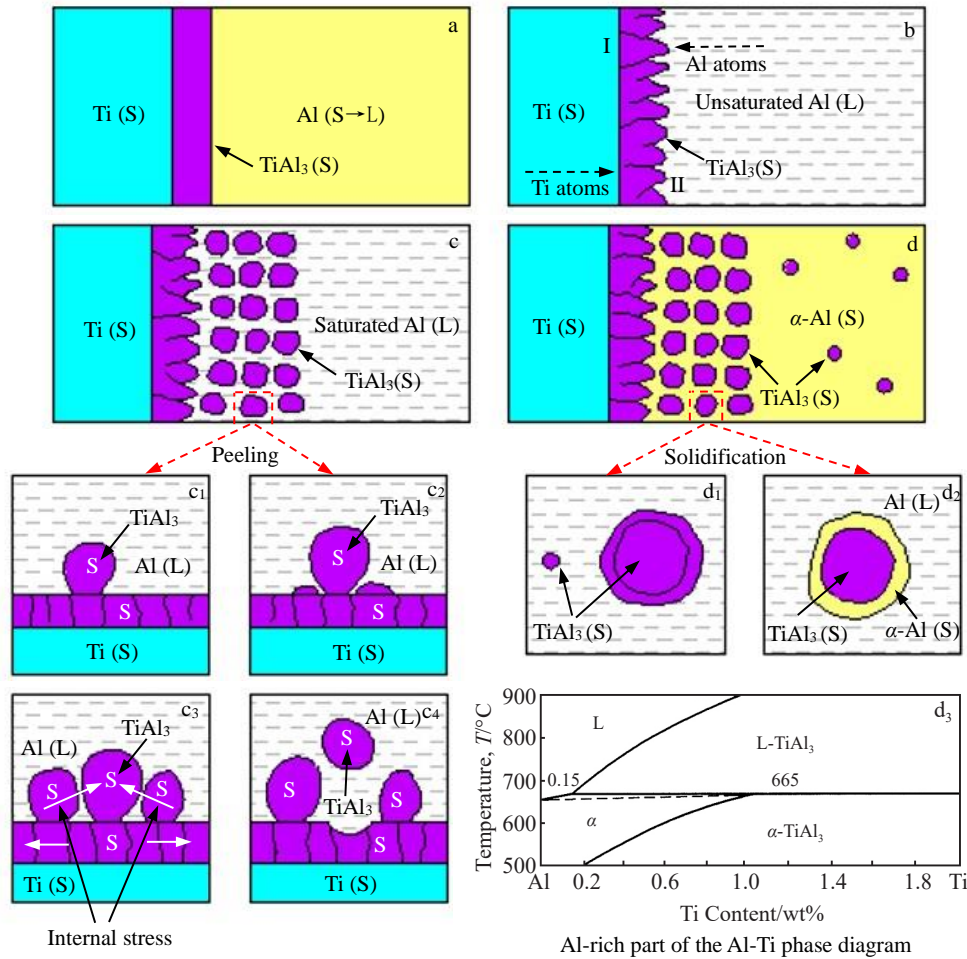


Fig.5 Formation mechanisms of interfacial layer in cold-rolled Ti/Al laminated composites during annealing: (a) formation of $TiAl_3$ phase by solid (S)-solid reaction between Ti and Al; (b) formation and dissolution of $TiAl_3$ phase by solid-liquid (L) reaction between Ti and unsaturated liquid Al; (c) formation of $TiAl_3$ phase by solid-liquid reaction between Ti and saturated liquid Al, and peeling-off procedure of $TiAl_3$ phase; (c₁) nucleation and spheroidization of $TiAl_3$ phase; (c₂) adjacent $TiAl_3$ regions forming at solid/liquid interface; (c₃) interaction of $TiAl_3$ spherules; (c₄) expulsion of $TiAl_3$ spherules; (d) phase transformation of saturated liquid Al during cooling; (d₁) precipitation of $TiAl_3$ phase from oversaturated liquid Al; (d₂) peritectic reaction between liquid Al and $TiAl_3$ phase to form α -Al solid solution; (d₃) Al-rich part of Ti-Al binary alloy phase diagram^[18]

725, and 750 °C, respectively)^[24]; S is the surface area of solid $TiAl_3$ in contact with liquid Al, which is set as the cross-sectional area of the specimen for simplicity with a dimension of 10 mm×15 mm; V is the volume of liquid Al bath, m³; ρ_{TiAl_3} is the density of $TiAl_3$ phase of 3369 kg/m³; φ is the content of Ti in $TiAl_3$ phase; k is the dissolution rate constant, m/s. For mass transfer with natural convection along the surface of vertical plate, k can be estimated roughly by Eq.(6)^[25] as follows:

$$Sh = 0.129 (Gr_{AB} Sc)^{1/3} \quad (6)$$

where Sh is the Sherwood number with $Sh=kL/D$ (L is the representative length, m; D is the diffusion coefficient through the liquid Al boundary layer, m²/s); Gr_{AB} is the Grashof number with $Gr_{AB}=gL^3\Delta\rho\rho_{Al}^2/\mu^2$ (g is the acceleration of gravity, 9.8 m/s²; $\Delta\rho$ is the buoyancy coefficient with $\Delta\rho=(\rho_L-\rho_{Al})/\rho_{Al}$; ρ_L is the density of saturated liquid Al alloy with Ti,

kg/m³; ρ_{Al} is the density of liquid Al bath; μ is the viscosity coefficient of liquid Al alloy); Sc is the Schmidt number with $Sc=\mu/D\rho_{Al}$. At 675, 700, 725, and 750 °C, the viscosity coefficient μ is 1.35×10⁻³, 1.30×10⁻³, 1.25×10⁻³, and 1.20×10⁻³ Pa·s, respectively^[26]. The diffusion coefficient D at 675, 700, 725, and 750 °C is 4.29×10⁻⁹, 4.83×10⁻⁹, 5.40×10⁻⁹, and 6.01×10⁻⁹ m²/s, respectively^[23]. L is the height of the specimen with a value of 0.015 m, ρ_{Al} is the density of pure Al with a value of 2.7×10³ kg/m³, and ρ_L can be estimated by Eq.(7)^[25] as follows:

$$1/\rho_L = c_s/\rho_{Ti} + (1 - c_s)/\rho_{Al} \quad (7)$$

where ρ_{Ti} is the density of pure Ti of 4.54×10³ kg/m³.

The relationship between the dissolved thickness of $TiAl_3$ phase and annealing time is shown in Fig.6a. The dissolution rate decreases with increasing the annealing time and reaches zero in a few minutes. Owing to the low solubility of Ti in liquid Al and the small amount of liquid Al, the dissolution thickness of $TiAl_3$ layer is merely a few microns. The Ti

content (c) in liquid Al can be expressed by Eq.(8)^[24], and the relationship between the Ti content in liquid Al and annealing time is shown in Fig.6b. The liquid Al bath is saturated within a few minutes. The higher the temperature, the shorter the time for liquid Al to reach saturation.

$$c = c_s \left[1 - \exp\left(-\frac{k_s t}{V}\right) \right] \quad (8)$$

2.2.3 Solid-liquid reaction between Ti and saturated Al

After the liquid Al is saturated, TiAl₃ phase ceases to dissolve, and then the growth of TiAl₃ phase can be described by Eq.(3). The newly formed TiAl₃ phase peels off from the TiAl₃/Al solid-liquid interface and migrates into liquid Al. This process continues until the liquid Al is entirely consumed, as shown in Fig.5c. It has been reported that the chemical reaction between Ti and Al is exothermic. When the exothermic energy is absorbed by TiAl₃ phase, after TiAl₃ phase is heated to the melting point (1623 K), part of the exothermic energy is still not consumed, which transforms the newly formed TiAl₃ phase into liquid^[27]. At a given reaction temperature T_r , the residual energy ΔH can be obtained by Eq.(9)^[28] as follows:

$$\Delta H = \Delta H_{T_r} - \int_{T_r}^{1623\text{K}} C_{\text{TiAl}_3(\text{s})} dT \quad (9)$$

where ΔH_{T_r} is the formation enthalpy of TiAl₃ phase at reaction temperature T_r , kJ/mol; $C_{\text{TiAl}_3(\text{s})}$ is the specific heat capacity of solid TiAl₃ phase in the temperature range of $T_r \sim 1623$ K, J/mol·K; T is the temperature. The value of ΔH_{T_r} is 181.02 kJ/mol when the reaction temperature is slightly higher than the melting point of Al^[29], and the value of $C_{\text{TiAl}_3(\text{s})}$ can be estimated by Eq.(10) with the data from Ref.[29]:

$$C_{\text{TiAl}_3(\text{s})} = 88.95 \times 4.41 \times 10^{-2} T - 9.95 \times 10^{-6} T^2 \quad (10)$$

Combining Eq. (9) and Eq. (10), the ΔH is calculated as 94.03, 97.09, 100.16, and 103.24 kJ/mol when the annealing temperatures are 675, 700, 725, and 750 °C, respectively. When ΔH is larger than the fusion enthalpy of TiAl₃ phase ΔH_m , the TiAl₃ phase melts. The value of ΔH_m cannot be found in the published literatures. If the difference between Ti and Al is neglected, the body-centered tetragonal crystal structure of TiAl₃ phase can be regarded as a deformed face-centered

cubic structure of Al with an elongation of 6.7% along the c direction and a contraction of 4.5% along the a and b directions^[30]. Hence, the fusion enthalpy of TiAl₃ phase can be estimated by the Richard rule^[31] as follows:

$$\frac{\Delta H_m}{T_m} = \Delta S_m \approx 8.372 \sim 16.744 \text{ (J/K)} \quad (11)$$

where ΔS_m is the fusion entropy of TiAl₃ phase. The value of ΔH_m is estimated in the range of 13.58~27.16 kJ/mol using the Richard rule, which is lower than the ΔH value. When the fusion enthalpy of TiAl₃ phase is 27.16 kJ/mol, and the specific heat capacity of liquid TiAl₃ phase is equal to that of solid TiAl₃ phase at 1623 K, the solid TiAl₃ phase melts by the residual energy ΔH and its adiabatic temperatures reach 2120.69, 2143.47, 2166.32, and 2189.24 K when the annealing temperatures are 675, 700, 725, and 750 °C, respectively. Therefore, when the exothermic energy is absorbed by TiAl₃ phase, the newly formed TiAl₃ particles transform into liquid. However, it is impossible for the exothermic energy to be completely absorbed by TiAl₃ phase. Part of the exothermic energy effectively dissipates to the surroundings, such as that of Ti, Al, and TiAl₃. Hence, the status of newly formed TiAl₃ phase depends on the actual exothermic energy absorbed by TiAl₃ phase. In this work, the thickness of TiAl₃ phase in cold-rolled Ti/Al laminated composites obeys a linear relationship with annealing time and the values of growth rate constant k_E are 2.98×10^{-8} , 4.80×10^{-8} , 5.76×10^{-8} , and 7.40×10^{-8} m/s at 675, 700, 725, and 750 °C, respectively. Meanwhile, the surroundings around the newly formed TiAl₃ phase have larger volume than the newly formed TiAl₃ phase does, and have high thermal conductivity (1.15, 86.36, and $21.9 \text{ W} \cdot \text{m}^{-1} \cdot \text{K}^{-1}$ for solid TiAl₃ phase, liquid Al, and solid Ti, respectively^[32-34]). Therefore, the exothermic energy is absorbed promptly by the surroundings around the newly formed TiAl₃ phase. Because the thermal conductivity of liquid Al is higher than that of solid Ti and TiAl₃ phase, the released heat transfers only through liquid Al by natural convection. The natural convection heat transfer coefficient h between TiAl₃ phase and liquid Al can be calculated by Eq.(12)^[34] as follows:

$$h = 0.902 \frac{\lambda}{L} \left[\frac{\text{Pr}}{0.861 + \text{Pr}} \right]^{1/4} \left(\frac{\text{Pr} \cdot \text{Gr}}{4} \right)^{1/4} \quad (12)$$

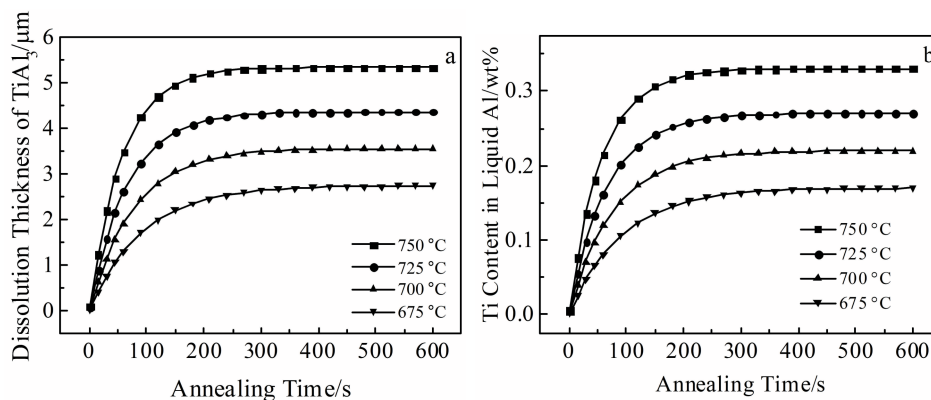


Fig.6 Dissolution thickness of TiAl₃ layer (a) and Ti content in liquid Al (b) versus annealing time

where λ is the thermal conductivity of liquid Al, $\text{W}\cdot\text{m}^{-1}\cdot\text{K}^{-1}$; Pr is the Prandtl number, $\text{Pr}=\nu/a$ (ν is the kinematic viscosity of liquid Al, m^2/s ; a is the thermal diffusivity of liquid Al, m^2/s); Gr is the Grashof number, $\text{Gr}=\beta g(T_s-T_\infty)L^3/\nu^2$ (β is the coefficient of volume expansion; T_s is the surface temperature of TiAl_3 phase; T_∞ is the temperature of the liquid Al far away from the surface of TiAl_3 phase). The values of λ , ν , and a can be set as constant roughly, and are equal to $86.36 \text{ W}\cdot\text{m}^{-1}\cdot\text{K}^{-1}$, $4.64\times 10^{-7} \text{ m}^2/\text{s}$, and $3.22\times 10^{-5} \text{ m}^2/\text{s}$, respectively^[34]. When the difference between T_s and T_∞ is in the range of $20\sim 1350 \text{ K}$, the calculated natural convection heat transfer coefficient h is in the range of $2000\sim 5000 \text{ W}\cdot\text{m}^{-2}\cdot\text{K}^{-1}$. The newly formed TiAl_3 thin layer can be considered as a lumped system when its thickness is in nanometer or micrometer scale, and the cooling time for the newly formed TiAl_3 layer with a thickness of δ can be calculated by Eq.(13)^[32] as follows:

$$t = \ln \left[\frac{T(t) - T_\infty}{T_0 - T_\infty} \right] \cdot \frac{\rho c \delta}{h} \quad (13)$$

where ρ is the density of TiAl_3 phase of $3.369\times 10^3 \text{ kg}/\text{m}^3$; c is the specific heat capacity of TiAl_3 phase; T_0 is the initial temperature of the newly formed TiAl_3 thin layer; $T(t)$ is the temperature of the newly formed TiAl_3 thin layer at time t ; δ is the thickness of the newly formed TiAl_3 thin layer. When the thickness of the newly formed TiAl_3 layer is $1 \mu\text{m}$ and the value of h is $2000 \text{ W}\cdot\text{m}^{-2}\cdot\text{K}^{-1}$, the cooling time from the adiabatic temperature of 2120.69 , 2143.47 , 2166.32 , and 2189.24 K to the melting temperature 1623 K is 124.95 , 133.15 , 141.60 , and $150.40 \mu\text{s}$ at 675 , 700 , 725 , and $750 \text{ }^\circ\text{C}$, respectively. Besides, the forming time of TiAl_3 layer of $1 \mu\text{m}$ in thickness is 33.56 , 20.83 , 17.36 , and 13.51 s at 675 , 700 , 725 , and $750 \text{ }^\circ\text{C}$, respectively. It can be seen from the calculation results that the exothermic energy during the formation of TiAl_3 phase quickly dissipates to the surroundings. Hence, it can be considered that the newly formed TiAl_3 phase only remains as liquid for a very short time.

Assuming that the newly formed TiAl_3 phase forms as a solid, the formation and peeling mechanisms of TiAl_3 particles in the interfacial layer are indicated in Fig.5c₁~5c₄. There are many fast diffusion channels during the interdiffusion of Ti and Al atoms through the TiAl_3 compact sub-layer, and then TiAl_3 phase forms at TiAl_3/Al and Ti/TiAl_3 interfaces (Fig.5c₁). The growth rate of the initial TiAl_3 nuclei decreases gradually with increasing the mass diffusion distance, and then the new TiAl_3 nuclei form near the initial TiAl_3 nuclei (Fig.5c₂). With the growth of TiAl_3 nuclei, the internal stress is generated owing to the molar volume difference between the products and the reactants (Fig.5c₃). In addition, the thermal stress may also play an important role^[35]. Due to the restricted ductility, TiAl_3 phase cracks, and some TiAl_3 particles separate from Ti and fall into liquid Al (Fig.5c₄).

2.2.4 Phase transformation of saturated liquid Al during cooling

When the annealed Ti/Al laminated composites are cooled in air, the unconsumed liquid Al solidifies (Fig.5d). As shown in the Al-rich part of the Ti-Al binary alloy phase diagram

(Fig.5d₃)^[18], TiAl_3 phase is precipitated from the oversaturated liquid Al since the solubility of Ti in liquid Al decreases with decreasing the temperature. Usually, the newly formed TiAl_3 phase is precipitated around the original TiAl_3 particles or other impurities (Fig. 5d₁). When the temperature reaches $665 \text{ }^\circ\text{C}$, a small amount of TiAl_3 phase and liquid Al form the α -Al solid solution through the peritectic reaction, as shown in Fig.5d₂. As the temperature decreases, the remaining liquid Al transforms into α -Al solid solution. With the further decrease in annealing temperature, the secondary TiAl_3 particles are precipitated from the oversaturated α -Al solid solution. Because the solubility of Ti in liquid Al is $0.17\text{wt}\%\sim 0.33\text{wt}\%$ at the temperature of $675\sim 750 \text{ }^\circ\text{C}$, the solidification of liquid Al and the precipitation of α -Al solid solution have little effect on the total amount of TiAl_3 phase in the interfacial layer.

2.3 Reaction kinetics between solid Ti and liquid Al

The average thicknesses of the interfacial layer in cold-rolled Ti/Al laminated composites annealed at $675\sim 750 \text{ }^\circ\text{C}$ for different time are shown in Table 3. It shows that the interfacial layer thickness increases with increasing the annealing temperature or annealing time in a certain range. Considering that the initial non-isothermal annealing stage is neglected, the dependence of the interfacial layer thickness at a given temperature on annealing time can be described by the empirical relationship of Eq.(14) or Eq.(15)^[16] as follows:

$$x=kt^n \quad (14)$$

$$\ln x = \ln k + n \ln t \quad (15)$$

where k is the growth rate constant; t is the annealing time; n is the kinetic exponent with $n=0.5$ for the growth governed by diffusion and $n=1$ for the growth governed by chemical reaction. The relationship between double logarithmic curves of the interfacial layer thickness x_i and annealing time is shown in Fig. 7a. Through the linear regression analysis, the values of the kinetic exponent n_i are 1.28 , 1.43 , 1.27 , and 1.23 at 675 , 700 , 725 , and $750 \text{ }^\circ\text{C}$, respectively. Here, the thicknesses of the interfacial layer annealed at different temperatures for 2 and 5 min are not used for linear regression analysis owing to the large deviation from the linear regression curves. The deviation can be attributed to the non-isothermal growth and dissolution of TiAl_3 phase at the initial annealing stage.

Assuming that all total cross-section areas of TiAl_3 phase in the interfacial layer are the same at different depths beneath the metallographic surface of the specimen, the volume fraction of TiAl_3 phase in the interfacial layer V_F can be replaced by the area fraction and expressed by Eq. (16) as follows:

$$V_F = \frac{S_c}{S_1} \quad (16)$$

where S_1 and S_c are the cross-section areas of the interfacial layer and TiAl_3 phase in the interfacial layer, respectively, and can be measured from SEM images using image processing software. Considering that the cross-sectional shape of all TiAl_3 particles is approximately rectangular, the dispersed TiAl_3 phase in the interfacial layer can be converted to an

Table 3 Experiment results of average thickness of interfacial layer x_i and equivalent thickness of $TiAl_3$ phase in interfacial layer x_E at different annealing temperatures and time (μm)

Annealing time/ min	Average thickness of interfacial layer, x_i				Equivalent thickness of $TiAl_3$ phase in interfacial layer, x_E			
	675 °C	700 °C	725 °C	750 °C	675 °C	700 °C	725 °C	750 °C
2	1.2	2	2.5	4.66	-	-	-	-
5	5.39	8.40	17.20	30.11	3.45	7.14	12.25	17.87
10	27.59	37.24	59.58	89.52	18.66	24.05	33.52	44.05
20	74.16	97.69	169.84	226.15	38.19	48.17	69.98	87.38
30	129.09	193.70	278.04	344.92	56.36	80.37	110.56	127.91
45	202.02	312.88	416.74	582.63	82.75	112.37	156.49	200.01
60	317.06	476.87	593.74	-	115.09	166.47	207.25	-
90	449.64	-	-	-	160.06	-	-	-

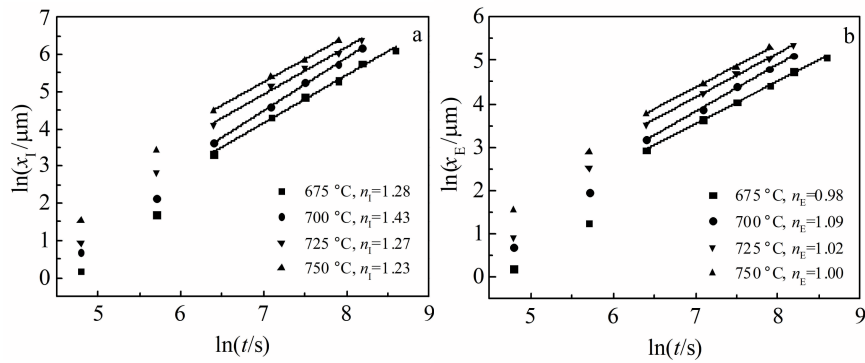


Fig.7 Double logarithmic curves of interfacial layer thickness (a) and equivalent thickness of $TiAl_3$ phase in interfacial layer (b) versus annealing time at different temperatures ($n_1=\ln x_i$, $n_E=\ln x_E$)

equivalent compact $TiAl_3$ layer, and the equivalent thickness of the $TiAl_3$ phase x_E can be obtained by Eq.(17) as follows:

$$x_E = V_F x_i \tag{17}$$

The equivalent thicknesses of $TiAl_3$ phase in the interfacial layer at different annealing temperatures and time are shown in Table 3. The double logarithmic curves of the equivalent thickness of $TiAl_3$ phase in the interfacial layer are shown in Fig.7b. Through linear regression analysis, the values of the kinetics exponent n_E are 0.98, 1.09, 1.02, and 1.00 at 675, 700, 725, and 750 °C, respectively, and all n_E values are very close to 1, indicating that the growth of $TiAl_3$ phase in the interfacial layer is governed by the chemical reaction because of the thin thickness and high diffusion coefficient of the $TiAl_3$ compact sub-layer which are directly proportional to the diffusion constant k_d [24]. Furthermore, the values of kinetics exponent n_1 larger than 1 are attributed to the fact that the volume fraction of $TiAl_3$ phase in the interfacial layer decreases with increasing the annealing time at different temperatures, as shown in Fig.8.

The relationships of the thickness of the interfacial layer and the equivalent thickness of $TiAl_3$ phase in the interfacial layer versus annealing time are shown in Fig. 9a and 9b, respectively. Through the linear regression analysis, the values of growth rate constant k_1 at 675, 700, 725, and 750 °C are 9.03×10^{-8} , 1.47×10^{-7} , 1.75×10^{-7} , and 2.33×10^{-7} m/s, respec-

tively; the values of growth rate constant k_E at 675, 700, 725, and 750 °C are 2.98×10^{-8} , 4.80×10^{-8} , 5.76×10^{-8} , and 7.40×10^{-8} m/s, respectively. Both k_1 and k_E obey the Arrhenius formula as follows[16]:

$$k_1 = k_{01} \exp\left(\frac{-Q_1}{RT}\right) \tag{18}$$

$$k_E = k_{0E} \exp\left(\frac{-Q_E}{RT}\right) \tag{19}$$

where k_{01} and k_{0E} are the pre-exponential factors, m/s; Q_1 and Q_E are the activation energies, kJ/mol; R is the gas constant,

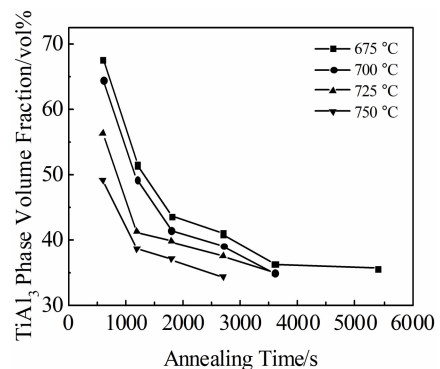


Fig.8 $TiAl_3$ phase volume fraction in interfacial layer versus annealing time at different temperatures

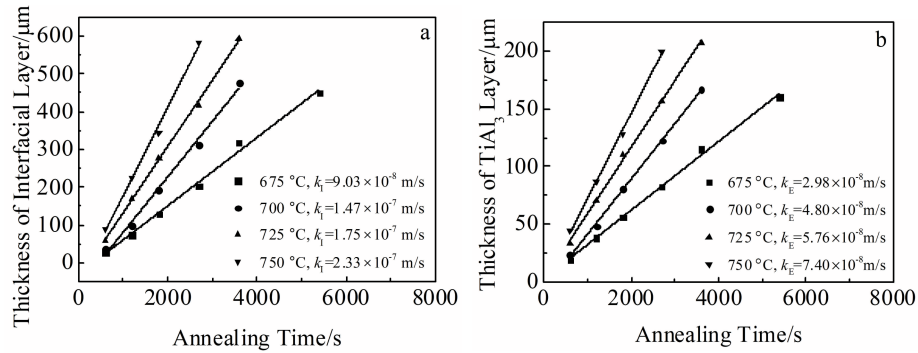


Fig.9 Thickness of interfacial layer (a) and equivalent thickness of TiAl_3 phase in interfacial layer (b) versus annealing time at different temperatures

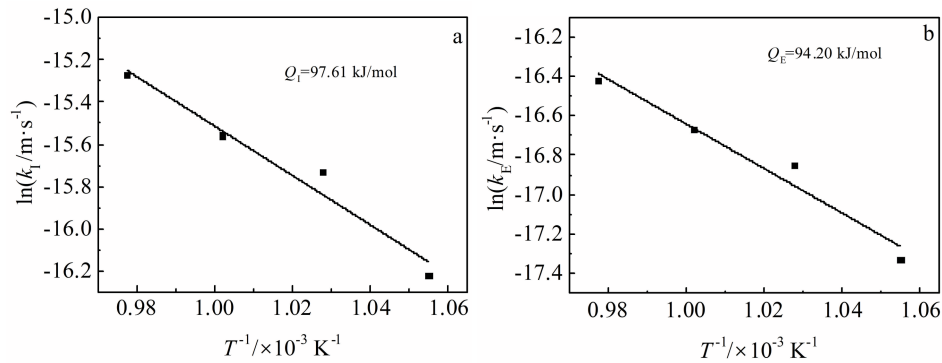


Fig.10 Arrhenius plots for growth of interfacial layer (a) and equivalent TiAl_3 phase layer (b)

Table 4 Reported and calculated values of activation energy of chemical reaction between solid Ti and liquid Al

Study focus	Temperature/K	Time/ks	Diffusion couple	Activation energy/kJ·mol ⁻¹	Ref.
Growth of Al+TiAl ₃	948~1023	0.12~5.4	99.6wt% Ti+99.5wt% Al	97.61	This work
Growth of TiAl ₃	948~1023	0.12~5.4	99.6wt% Ti+99.5wt% Al	94.20	This work
Dissolution of Ti	973~1193	5.4~32.4	99.75wt% Ti+99.99wt% Al	92.4±8.4	[13]
Growth of Al+TiAl ₃	973~1193	5.4~32.4	99.75wt% Ti+9.99wt% Al	96.6±8.4	[13]
Growth of Al+TiAl ₃	973~1173	2.25~38.1	Ti in Ti-saturated Al matrix	127.60±29.66	[36]
Growth of TiAl ₃	973~1173	0.9~14.4	99.9wt% Ti+99.99wt% Al	14.93	[12]
Growth of Al+TiAl ₃	973~1173	0.9~14.4	99.9wt% Ti+99.99wt% Al	15.7	[12]

$8.314 \text{ J} \cdot \text{mol}^{-1} \cdot \text{K}^{-1}$; T is the absolute temperature, K. The values of Q_1 and Q_E can be obtained by the plots of $\ln k_i$ and $\ln k_E$ versus the reciprocal of temperature $T^{-1} \times 10^{-3}$, respectively, as shown in Fig. 10. Through linear regression analysis, the values of Q_1 and Q_E are 97.61 and 94.20 kJ/mol, respectively.

The reported values of the activation energy for the chemical reaction between solid Ti and liquid Al are summarized in Table 4. As shown in Table 4, the activation energies in this work are consistent with those in Ref.[13] and slightly lower than that in Ref.[36]. The activation energies in Ref.[12] are much lower than those obtained by other researchers, which is attributed to the following reasons. (1) Due to the shorter annealing time, the larger volume of liquid Al and the higher concentration of Ti in liquid Al, at 900 °C, the dissolution of TiAl_3 phase has a great influence on the amount

of TiAl_3 phase and the thickness of the interfacial layer. (2) There is a longer incubation period at lower temperatures (700 and 800 °C) owing to the oxide films in Ref. [12], which results in a great error in the calculation of the growth rate constants and activation energies.

3 Conclusions

1) The interfacial layer between Ti and Al consists of two sub-layers: a thin compact TiAl_3 sub-layer and a granular TiAl_3 sub-layer. The thickness of the compact TiAl_3 sub-layer is almost unchanged at different temperatures or time, but the thickness of the granular sub-layer increases with increasing the annealing time or annealing temperature.

2) The formation mechanism of the interfacial layer and a simplified method for transformation of the dispersed TiAl_3

phase in the interfacial layer to an equivalent compact TiAl_3 layer were successfully established. The growth of the equivalent TiAl_3 layer is governed by chemical reaction. The thickness of the equivalent TiAl_3 layer obeys a linear relationship with annealing time, and the activation energy for the growth of the equivalent TiAl_3 layer is 94.20 kJ/mol.

References

- Peng L M, Li H, Wang J H. *Materials Science and Engineering A* [J], 2005, 406(1-2): 309
- Shen Zhengzhang, Lin Junpin, Liang Yongfeng et al. *Rare Metals*[J], 2016, 35(1): 1
- Assari A H, Eghbali B. *Journal of Alloys and Compounds*[J], 2019, 773: 50
- Foadian F, Soltanieh M, Adell M et al. *Metallurgical and Materials Transactions B*[J], 2016, 47(5): 2931
- Li Hongxiang, Nie Xinyu, He Zanbing et al. *Metallurgy and Materials*[J], 2017, 24(12): 1412
- Gurevich L, Pronichev D, Trunov M. *IOP Conference Series: Materials Science and Engineering*[J], 2016, 116(1): 12 011
- Jiang Shuying, Li Shichun, Zhang Lei. *Transactions of Non-ferrous Metals Society of China*[J], 2013, 23(12): 3545
- Maryam Y, Hamid D. *Journal of Alloys and Compounds*[J], 2018, 766: 721
- Chen Gang, Song Xiaoguo, Hu Nan et al. *Journal of Alloys and Compounds*[J], 2017, 694: 539
- Liu Zhiwei, Han Qingyou, Li Jianguo. *Powder Technology*[J], 2013, 247: 55
- Mackowiak J, Shreir L L. *Journal of the Less-Common Metals* [J], 1959, 1(6): 456
- Sujata M, Bhargava S, Suwas S et al. *Journal of Materials Science Letters*[J], 2001, 20(24): 2207
- Mackowiak J, Shreir L L. *Journal of the Less-Common Metals* [J], 1968, 15(3): 341
- Jiang Shuying, Li Shichun. *Rare Metal Materials and Engineering* [J], 2011, 40(6): 983
- Gurevich L M, Shmorgun V G. *Metallurgist*[J], 2016, 59(11-12): 1221
- Nie X Y, Liu J C, Li H X et al. *Materials and Design*[J], 2014, 63: 142
- Assari A H, Eghbali B. *Metals and Materials International*[J], 2016, 22(5): 915
- Schuster J C, Palm M. *Journal of Phase Equilibria and Diffusion* [J], 2006, 27(3): 255
- Araújo L L, Behar M. *Applied Physics A*[J], 2000, 71(2): 169
- Wöhlert S, Bormann R. *Journal of Applied Physics*[J], 1999, 85(2): 825
- Gusak A M. *Diffusion-Controlled Solid State Reactions*[M]. Weinheim: Wiley-VCH Press, 2010
- Li L, Nagai K, Yin F. *Science and Technology of Advanced Materials*[J], 2008, 9(2): 23 001
- Du Y, Chang Y A, Huang B Y et al. *Materials Science and Engineering A*[J], 2003, 363(1-2): 140
- Dybkov V I. *Reaction Diffusion and Solid State Chemical Kinetics*[M]. Kyiv: IPMS Publications, 2010: 212
- Katayama H G, Momono T, Doe M et al. *ISIJ International*[J], 2007, 34(2): 171
- Schick M, Brillo J, Egry I et al. *Journal of Materials Science*[J], 2012, 47(23): 8145
- Harach D J, Vecchio K S. *Metallurgical and Materials Transactions A*[J], 2001, 32(6): 1493
- Sujata M, Bhargava S, Suwas S et al. *Metals Materials and Process*[J], 2006, 18(4): 283
- Barin I. *Thermochemical Data of Pure Substances*[M]. New York: VCH Publishers, 1995
- Tardy J, Tu K N. *Physical Review B*[J], 1985, 32(4): 2070
- Xu Zuyao, Li Lin. *Material Thermodynamics*[M]. Beijing: Science Press, 2004: 22 (in Chinese)
- Cengel Y A. *Heat Transfer: A Practical Approach*[M]. Beijing: Higher Education Press, 2007
- Duan Y H, Sun Y, Lu L. *Computational Materials Science*[J], 2013, 68: 229
- Lin Bainian, Wei Zunjie. *Transfer Principle of Metal Hot Forming*[M]. Harbin: Harbin Institute of Technology Press, 2000
- Sujata M, Bhargava S, Sangal S. *ISIJ International*[J], 2007, 36(3): 255
- Eremenko V N, Natanzon Y V, Petrishchev V Y. *Powder Metallurgy and Metal Ceramics*[J], 1987, 26(2): 118

冷轧 Ti/Al 层状复合材料固-液反应过程中的界面微观组织演变

张建宇¹, 赵小佳², 王艳辉¹, 陈庆安¹, 李河宗¹, 陈亚宇¹

(1. 河北工程大学 机械与装备工程学院, 河北 邯郸 056038)

(2. 邯郸学院 河北省杂环化合物重点实验室, 河北 邯郸 056005)

摘要: 将冷轧 Ti/Al 层状复合材料在 675~750 °C 下进行不同时间的退火处理, 退火过程中钛和铝都保持过剩, 研究了 Ti/Al 层状复合材料的界面微观组织演变。结果表明: Ti 和 Al 的界面层由 2 个亚层组成, 其中一个为紧密的 TiAl_3 亚层, 其微观结构为紧密的 TiAl_3 层, 其中分布着随机取向的充满 Al 的裂纹, 另一个为颗粒状的 TiAl_3 亚层, 其微观组织结构是颗粒状的 TiAl_3 分布在 Al 基体中。在不同的退火温度和时间条件下, 紧密 TiAl_3 亚层的厚度几乎没有变化, 但是颗粒状亚层的厚度随着退火温度及时间的增加而增加; 另外, 界面层中的 TiAl_3 颗粒的体积分数在不同的温度下均随着退火时间的延长而下降。因此提出了反应扩散模型来描述界面层的形成机理, 在此模型中, TiAl_3 相是化学反应和扩散的结果, 并且也考虑了 TiAl_3 相的溶解。计算结果表明 TiAl_3 相的形成与生长由化学反应控制, 其等效厚度与退火时间之间遵循线性规律, 这主要是因为 Ti 和 Al 原子能够快速通过紧密的薄 TiAl_3 亚层。

关键词: 微观组织演变; 固-液反应; Ti/Al 层状复合材料; 动力学